Extended x-ray-absorption fine-structure study of $GaAs_xP_{1-x}$ semiconducting random solid solutions

Zhonghua Wu and Kunquan Lu
Institute of Physics, Chinese Academy of Sciences, Beijing 100080, China

Yuren Wang
University of Science and Technology Beijing, Beijing 100083, China

Jun Dong, Hefeng Li, and Chenxi Li
Institute of Physics, Chinese Academy of Sciences, Beijing 100080, China

Zhengzhi Fang
University of Science and Technology Beijing, Beijing 100083, China
(Received 16 July 1992; revised manuscript received 23 March 1993)

The extended x-ray-absorption fine-structure (EXAFS) technique is employed to probe the local atomic structure of the III-V pseudobinary solid solutions $GaAs_xP_{1-x}$ as a function of the composition. The first- and second-neighbor bond lengths as well as their variation with the composition are reported. The results imply that the local atomic structure is distorted. Both first-neighbor bond lengths and cation-cation bond lengths exhibit a bimodal structure, showing a tendency to retain the values of pure compounds. Anion-anion bond lengths are much closer to those predicted by Vegard's law; however they still show a significant deviation from it. On the basis of this result, the authors propose that the atomic-scale structure of these compounds can be described by a random distribution of five special coordination tetrahedra. The relation between local atomic structure and EXAFS as well as x-ray-diffraction results is discussed.

I. INTRODUCTION

$GaAs_xP_{1-x}$ ($x=0,1$) are typical III-V pseudobinary semiconducting alloys and form completely miscible solid solutions for the whole range of x. They are covalently bonded and belong to the $F\bar{4}3m$ space group with a zinc-blende structure. Their smallest structural units are tetrahedra: when cations occupy the vertices of the tetrahedra, then anions are situated randomly in the centers and vice versa.

$GaAs_xP_{1-x}$ solid solutions have wide application in industry. Their energy gaps[1] and emitted wave lengths[2] vary continuously with composition and with the degree of disorder.[3] The electrical properties of $GaAs_xP_{1-x}$ superlattices are strongly influenced by internal stress due to lattice mismatch.[4–7] Information on crystal structure and atomic arrangement in these solid solutions is very useful in order to understand the above features.

However, the atomic-scale structure of $GaAs_xP_{1-x}$ solid solutions and other III-V pseudobinary semiconducting materials is still insufficiently known to quantitatively predict its effect on the physical properties of the alloys. Extended x-ray-absorption fine structure (EXAFS) can provide more detailed near-neighbor atomic-structure information than conventional x-ray diffraction. Although some authors have studied the structures of several semiconducting solid solutions with different composition,[8–11] the investigation of $GaAs_xP_{1-x}$ is still not complete. T. Sasaki *et al.*[12] studied the $GaAs_xP_{1-x}$ system with EXAFS, showing the tendency of bond lengths to vary with composition, but only the first coordination shells were analyzed and the results were incomplete. Therefore, more accurate measurements and further study on $GaAs_xP_{1-x}$ are needed because of its importance in applications.

In this paper a study of the local atomic structure of $GaAs_xP_{1-x}$ solid solutions with EXAFS is presented and more detailed structural information is given. The experiments are described in Sec. II, a brief illustration about data analysis is given in Sec. III, the results and discussions are in Sec. IV, and the conclusions are in Sec. V.

II. EXPERIMENTAL

Homogeneous solid solutions of $GaAs_xP_{1-x}$ were formed by solid-state interdiffusion[4] between powders of GaAs and GaP mixed in the following ratios: $X=0.11$, 0.25, 0.49, 0.79, 0.93. The conditions of the thermal treatment are listed in Table I. All the samples were furnace cooled to room temperature. Phase homogeneity was checked by x-ray diffraction. A quantitative chemical analysis verified the compositions of the solid solutions and indicated that the relative error of the atomic ratio between As and P in every sample is not larger than $\pm 3\%$. The lattice parameters of the solid solutions measured by x-ray diffraction are also presented in Table I. They follow Vegard's law as described in Ref. 13.

The samples were ground into powders (finer than 380

TABLE I. Lattice parameters (in Å) of $GaAs_xP_{1-x}$ solid solutions and the thermal treatment time (in days). The lattice parameters were measured at room temperature; the thermal treatments were performed in vacuum-sealed quartz ampoules.

Composition X	0.0	0.11	0.25	0.49	0.79	0.93	1.0
Lattice parameter	5.454	5.477	5.508	5.562	5.626	5.644	5.659
1000 °C		4	2				
900 °C		5	5		3	3	
850 °C		8	8	7	11	11	

mesh) and smeared on Scotch tape homogeneously; several layers were folded to reach the optimum thickness $\mu d \simeq 2$. EXAFS measurements were made at the BL-10B beamline of the Photon Factory in Japan with a channel-cut Si(311) monochromator. The storage ring was run at 2.5 Gev with a current of about 240–290 mA. At least two scans of Ga and As K absorption for each sample were taken independently at 80 K. The photon energy E was calibrated by using the Cu K absorption edge at 8980.3 eV. The energy resolution was about 2 eV at the K-absorption edges of Ga and As. Two ionization chambers were used to detect the photon intensities I_0 and I simultaneously in front of and behind the sample. The detectors were filled with a gas mixture of Ar and N_2. Higher-order harmonics were eliminated by adjusting the ratios of the mixed gases and the lengths of the detectors. The ranges of the measured spectra were all from 500 eV below the absorption edge to more than 1100 eV above it. The collecting time for each data point was 1 sec. In addition, three scans for every absorption edge were also collected at the newly built 4W1B beamline of the Synchrotron Radiation Laboratory of BEPC, Institute of High Energy Physics, Chinese Academy of Sciences, and the results are consistent with those obtained at the Photon Factory.

III. DATA ANALYSIS

The common data-analysis procedure[14] was adopted. The EXAFS oscillations can be written as

$$\chi(k)=\sum_j \frac{N_j}{kR_j^2} A_j(\pi,k,R_j)\sin[2kR_j+\Phi_j(\pi,k,R_j)] , \quad (1)$$

where

$$A_j(\pi,k,R_j)=S_0^2 F_j(\pi,k,R_j)\exp(-2k^2\sigma_j^2) \times \exp\left[\frac{-2R_j}{\lambda_j}\right] , \quad (2)$$

N_j is the jth shell coordination number, $F_j(\pi,k,R_j)$ is the backscattering amplitude, $\Phi_j(\pi,k,R_j)$ is the phase shift and σ_j^2 is the mean-square displacement of the distance R_j of the jth shell atoms. λ_j is the mean free path of the photoelectrons.

The EXAFS functions $\chi(k)$ were extracted from the experimental spectra by subtracting the backgrounds, the single-atom absorptions, and by normalizing with the edge jumps. The Fourier-transform spectra of $k\chi(k)$ between 2.10 and 16.98 $Å^{-1}$ are shown in Figs. 1 and 2 for the As and Ga K absorption, respectively. The first- and second-neighbor isolated EXAFS spectra $k\chi_1(k)$ and $k\chi_2(k)$ were obtained with the technique of Fourier filtering, the ranges of which are approximately 1.2–2.6 Å for the first shells and 3.0–4.1 Å for the second shells. The number of independent points ($N_{\rm pts}=2\Delta k\Delta R/\pi$) (Ref. 15) are always between 8 and 12, allowing one to perform two-shell fittings. As an example, the $k\chi_1(k)$ spectrum of As K absorption of $GaAs_{0.79}P_{0.21}$ sample is shown in Fig. 3.

Two compounds GaAs and GaP are used as standard samples and their EXAFS spectra were collected and analyzed in the same condition as the unknown samples. At room temperature, the lattice parameters of GaAs and GaP are 5.659 and 5.454 Å, respectively. The backscattering amplitudes and phase shifts of the first coordination shells (Ga-As, Ga-P, As-Ga) and of the second coordination shells (Ga-As-Ga, Ga-P-Ga, As-Ga-As) can be extracted directly from the standard samples GaAs and GaP. However, those of the second coordinating atom pair As-Ga-P of As atoms in the solid solutions, which cannot be directly extracted from the standards, were obtained from

$$A_{\text{As-Ga-P}} = A^{\rm Exp}_{\text{As-Ga-As}}(A^T_{\text{As-Ga-P}}/A^T_{\text{As-Ga-As}}) , \quad (3)$$

$$\Phi_{\text{As-Ga-P}}=\Phi^{\rm Exp}_{\text{As-Ga-As}}+(\Phi^T_{\text{As-Ga-P}}-\Phi^T_{\text{As-Ga-As}}) . \quad (4)$$

Here, $A^{\rm Exp}_{\text{As-Ga-As}}$ and $\Phi^{\rm Exp}_{\text{As-Ga-As}}$ are the amplitude and phase shift extracted from the standard sample GaAs. $A^T_{\text{As-Ga-As}}$, $A^T_{\text{As-Ga-P}}$ and $\Phi^T_{\text{As-Ga-As}}$, $\Phi^T_{\text{As-Ga-P}}$ are amplitudes and phase shifts calculated with curved-wave theory.[16]

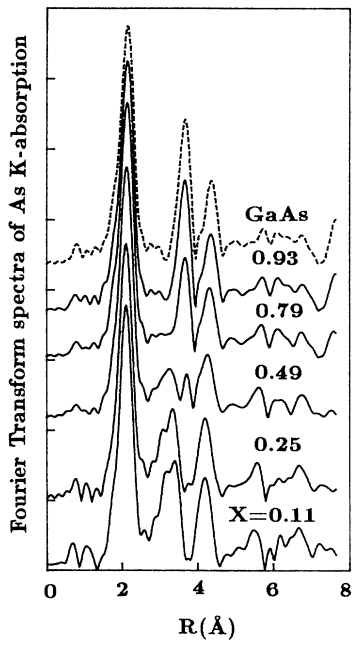

FIG. 1. Fourier-transform spectra of As K absorption in $GaAs_xP_{1-x}$ solid solution (80 K).

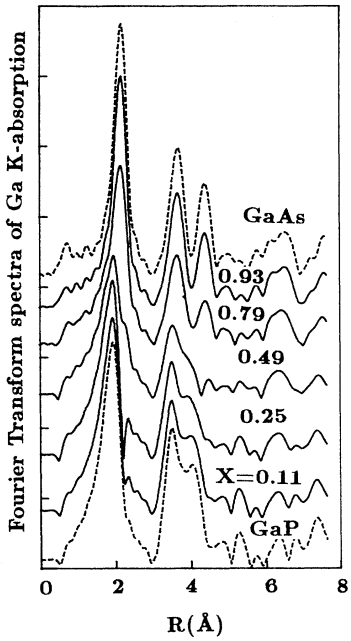

FIG. 2. Fourier-transform spectra of Ga K absorption in $GaAs_xP_{1-x}$ solid solution (80 K).

As an example, the fitting spectrum in k space for the $GaAs_{0.79}P_{0.21}$ is shown in Fig. 3.

The fitting parameters are listed in Tables II, III, and IV, respectively. The first- and second-neighbor bond lengths, as well as their fitting curves, are shown in Figs. 4, 5, and 6, respectively. Errors are estimated by using the method recommended by the International Standards and Criteria on XAFS.[15]

Figure 2 shows that the second-neighbor peaks around Ga are strongly overlapped with third neighbor for $X \leq 0.5$, and the former is dominant. The procedure used to separate the second-neighbor peaks is as follows. We tried extracting χ_2 and χ_3 by isolating the second peak and the third one, respectively, then transforming $\chi_2+\chi_3$

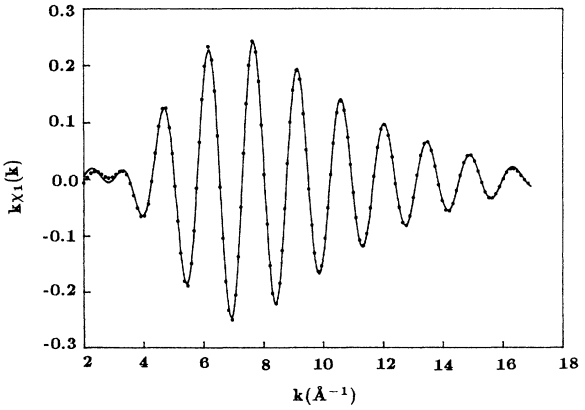

FIG. 3. K-absorption Fourier-filter spectrum and its fitting curve of the first neighbor of As with $x=0.79$ (80 K) ($\cdots$, experimental value; ——, fitting curve).

TABLE II. First-near-neighbor coordination parameters of $GaAs_xP_{1-x}$ solid solutions (80 K). (1) The coordination number N is the weighted average value over every possible coordination; (2) due to the contraction of lattice parameters with the temperature from 300 to 80 K, the first-neighbor bond lengths of standard samples $R_{Ga\text{-}As}=2.446$ Å and $R_{Ga\text{-}P}=2.359$ Å; (3) $\Delta\sigma^2=\sigma_u^2-\sigma_s^2$; subscripts u and s represent unknown and standard sample, respectively.

Samples	$N_{As\text{-}Ga}$	$N_{Ga\text{-}As}$	$N_{Ga\text{-}P}$	$R_{As\text{-}Ga}$ (Å)	$R_{Ga\text{-}As}$ (Å)	$R_{Ga\text{-}P}$ (Å)	$\Delta\sigma^2_{As\text{-}Ga}$ (10^{-3} Å^2)	$\Delta\sigma^2_{Ga\text{-}As}$ (10^{-3} Å^2)	$\Delta\sigma^2_{Ga\text{-}P}$ (10^{-3} Å^2)
$GaAs_{0.11}P_{0.89}$	4.1±0.4	0.4±0.3	3.6±0.3	2.42_7±0.015	2.43_1±0.015	2.36_1±0.010	−0.4±0.5	0.1±1.0	0.2±1.0
$GaAs_{0.25}P_{0.75}$	4.1±0.4	1.0±0.4	3.1±0.3	2.42_8±0.010	2.43_3±0.010	2.36_2±0.010	−0.3±0.5	0.7±2.0	0.5±1.0
$GaAs_{0.49}P_{0.51}$	4.0±0.4	2.0±0.3	2.0±0.2	2.43_6±0.010	2.43_5±0.010	2.36_6±0.010	−0.3±0.5	0.2±1.0	0.2±1.0
$GaAs_{0.79}P_{0.21}$	4.0±0.4	3.2±0.3	0.9±0.3	2.44_1±0.010	2.44_2±0.010	2.36_9±0.010	−0.3±0.5	0.3±0.5	0.4±3.0
$GaAs_{0.93}P_{0.07}$	4.0±0.4	3.7±0.4	0.3±0.2	2.44_4±0.010	2.44_5±0.010	2.37_2±0.015	−0.2±0.5	−0.1±0.5	0.2±5.0

TABLE III. Second-near-neighbor coordination parameters of Ga K absorption in $GaAs_xP_{1-x}$ solid solutions (80 K). The second-neighbor bond lengths of standard samples $R_{Ga\text{-}As\text{-}Ga}=3.996$ Å and $R_{Ga\text{-}P\text{-}Ga}=3.852$ Å at low temperature 80 K; the coordination numbers and Debye-Waller factor have the same meaning as in Table II.

Samples	$N_{Ga\text{-}As\text{-}Ga}$	$N_{Ga\text{-}P\text{-}Ga}$	$R_{Ga\text{-}As\text{-}Ga}$ (Å)	$R_{Ga\text{-}P\text{-}Ga}$ (Å)	$\Delta\sigma^2_{Ga\text{-}As\text{-}Ga}$ (10^{-3} Å^2)	$\Delta\sigma^2_{Ga\text{-}P\text{-}Ga}$ (10^{-3} Å^2)
$GaAs_{0.11}P_{0.89}$	1.4±1.0	10.7±0.4	3.95_4±0.020	3.85_6±0.010	−0.1±6.0	0.2±0.8
$GaAs_{0.25}P_{0.75}$	3.0±0.6	9.0±0.4	3.95_9±0.010	3.86_2±0.005	0.3±2.0	0.4±0.5
$GaAs_{0.49}P_{0.51}$	5.8±0.2	6.1±0.2	3.97_0±0.005	3.87_1±0.005	−0.2±0.2	0.4±0.2
$GaAs_{0.79}P_{0.21}$	9.5±0.4	2.6±0.4	3.98_4±0.005	3.88_1±0.015	0.4±0.3	0.3±0.5
$GaAs_{0.93}P_{0.07}$	11.2±1.0	0.9±0.8	3.99_1±0.005	3.88_8±0.030	0.1±0.5	0.1±4.0

to real space, and comparing the transformed peak shape with that in Fig. 2. We repeated this procedure until the Fourier-transformed peak of $\chi_2+\chi_3$ was coincident with the initial overlapped one in Fig. 2. Fitting these χ_2, the structural parameters of the second shell around Ga were obtained as listed in Table III. We also performed a four-shell [Ga-P-Ga, Ga-As-Ga, Ga-(As,P)-Ga-P, and Ga-(As,P)-Ga-As] fitting with theoretical amplitudes and phaseshifts[16] on the signal obtained by backtransforming both second and third peaks. The results also confirmed the values listed in Table III.

IV. RESULTS AND DISCUSSION

A. The first-neighbor shell

Since coordination numbers obtained are proportional to concentrations, we deduce that the solid solutions are complete miscible disordered ones and there is no evidence of chemical short-range order or segregation.

From Table II we observe that bond lengths of the As-Ga atom pair measured from the As K absorption agree with those of the Ga-As atom pair from the Ga K absorption. Figure 4 shows that bond lengths $R_{Ga\text{-}As}$ (equal to $R_{As\text{-}Ga}$) and $R_{Ga\text{-}P}$ increase linearly with increasing composition with a similar slope S_1: the distance between the two subshells (Ga-As, Ga-P) is almost fixed ($\simeq$0.07 Å). The ratio S_1/S_1^V is about 18% (S_1^V is the slope of the first coordination bond length described with Vegard's law). It means that in $GaAs_xP_{1-x}$ solid solutions there is a large deviation from the ideal lattice atomic positions. Namely, the interatomic distances do not vary as much as those calculated from the lattice parameter. Therefore, directly using the virtual-crystal approximation (VCA) model to describe the atomic-neighbor bond lengths is incorrect.

Obviously, S_1/S_1^V related to type of bond, crystal structure, and atomic type in solid solutions. For different types of solid solutions, it is different. For ionic and covalent solid solutions, S_1/S_1^V is independent of composition and, as claimed by Boyce and Mikkelsen,[17] about 40% in the former and about 20% in the latter. But for metallic solid solutions, it is composition dependent. Namely, the first-neighbor bond lengths do not linearly change with composition X in those solid solutions.[18]

B. The second-neighbor shell

As for the second-neighbor coordination around Ga, the bond lengths $R_{Ga\text{-}As\text{-}Ga}$ and $R_{Ga\text{-}P\text{-}Ga}$ vary linearly with composition, have the same slope S_2, and the difference between the two bond lengths is about 0.1 Å with $S_2/S_2^V\simeq 30\%$ (Fig. 5). On the other hand, the two subshells ($R_{As\text{-}Ga\text{-}As}$ and $R_{As\text{-}Ga\text{-}P}$) around the As atom have a stronger tendency to follow Vegard's law. In fact, in this case $S_2'/S_2^V\simeq 65\%$. In order to maintain long-range order, as confirmed by x-ray diffraction, the weighted average bond length over $R_{As\text{-}Ga\text{-}As}$, $R_{As\text{-}Ga\text{-}P}$, and $R_{P\text{-}Ga\text{-}P}$ must follow Vegard's law. Therefore, $S_{As\text{-}Ga\text{-}As}+S_{P\text{-}Ga\text{-}P}=2S_{As\text{-}Ga\text{-}P}$. We have calculated $S_{P\text{-}Ga\text{-}P}$ and the bond length $R_{P\text{-}Ga\text{-}P}$ as shown in Fig. 6 and Table IV.

TABLE IV. Second-near-neighbor coordination parameters of As K absorption in $GaAs_xP_{1-x}$ solid solutions (80 K). (1) The second-neighbor bond lengths of standard samples $R_{As\text{-}Ga\text{-}As}=3.996$ Å and $R_{P\text{-}Ga\text{-}P}=3.852$ Å. Approximately, $R_{As\text{-}Ga\text{-}P}=(R_{As\text{-}Ga\text{-}As}+R_{P\text{-}Ga\text{-}P})/2=3.924$ Å as used in Eqs. (3) and (4); (2) The coordination numbers and Debye-Waller factors have the same meaning as in Table II; (3) $R_{P\text{-}Ga\text{-}P}$ are the evaluated values.

Samples	$N_{As\text{-}Ga\text{-}As}$	$N_{As\text{-}Ga\text{-}P}$	$R_{As\text{-}Ga\text{-}As}$ (Å)	$R_{As\text{-}Ga\text{-}P}$ (Å)	$R_{P\text{-}Ga\text{-}P}$ (Å)	$\Delta\sigma^2_{As\text{-}Ga\text{-}As}$ (10^{-3} Å^2)	$\Delta\sigma^2_{As\text{-}Ga\text{-}P}$ (10^{-3} Å^2)
$GaAs_{0.11}P_{0.89}$	1.3±1.0	10.7±1.0	3.91_2±0.040	3.88_8±0.030	3.86_4	0.0±6.0	0.0±2.0
$GaAs_{0.25}P_{0.75}$	3.1±0.8	9.1±0.6	3.92_5±0.020	3.90_3±0.030	3.88_0	1.6±2.0	1.6±1.0
$GaAs_{0.49}P_{0.51}$	6.0±0.7	6.1±0.6	3.94_7±0.010	3.92_5±0.030	3.90_6	1.0±1.0	1.9±0.5
$GaAs_{0.79}P_{0.21}$	9.6±0.8	2.6±0.6	3.97_4±0.010	3.95_3±0.030	3.94_0	0.2±0.5	1.5±5.0
$GaAs_{0.93}P_{0.07}$	11.2±0.8	0.8±0.4	3.98_9±0.005	3.97_5±0.040	3.95_5	0.0±0.3	0.2±6.0

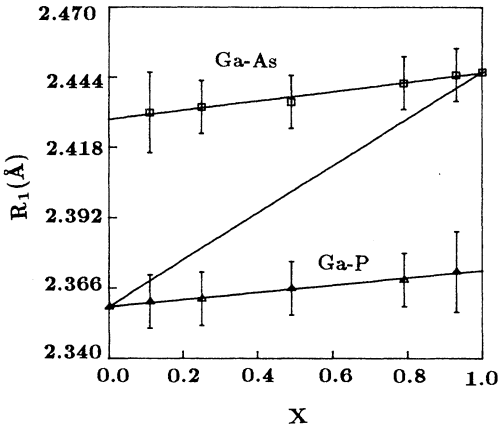

FIG. 4. First-neighbor bond lengths of $GaAs_xP_{1-x}$ solid solution. Symbols denote the experimental results. The upper solid line is the fitting curve of $R_{Ga\text{-}As}$ and the lower solid line is the fitting curve of $R_{Ga\text{-}P}$. The middle line is the value indicated by VCA.

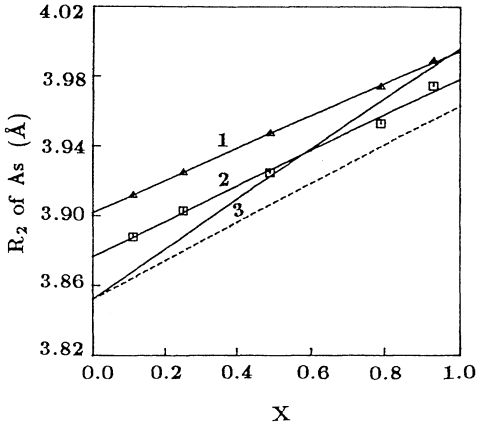

FIG. 6. Second-neighbor bond lengths of As in $GaAs_xP_{1-x}$ solid solution. Symbols denote the experimental results and the solid lines are the fitting curves. (1) $R_{As\text{-}Ga\text{-}As}$; (2) $R_{As\text{-}Ga\text{-}P}$; (3) the value indicated by VCA. The dotted line is the evaluated value of $R_{P\text{-}Ga\text{-}P}$.

C. The local atomic-structure model

Synthesizing the instructural information on bond lengths, we see that in the lattice of $GaAs_xP_{1-x}$ solid solutions, the Ga sublattice is relatively rigid while the mixed sublattice (consisting of As and P atoms) is more flexible relative to that in GaP and GaAs compounds. The feature of this distortion can be observed directly from the Fourier transform spectra in Figs. 1 and 2. In the cases having a Ga central atom, the second coordination peaks that contain Ga atoms are more stable while the third ones change greatly with composition. Moreover, the case having an As central atom presents a striking contrast with that of the Ga central atom. Based on our and other[8–11] results on pseudobinary III-V or II-IV solid solutions, the conclusion is that the mixed sublattice composed of displaceable atoms approaches the VCA model, but the other sublattice tends to maintain the same structure as in pure end compounds.

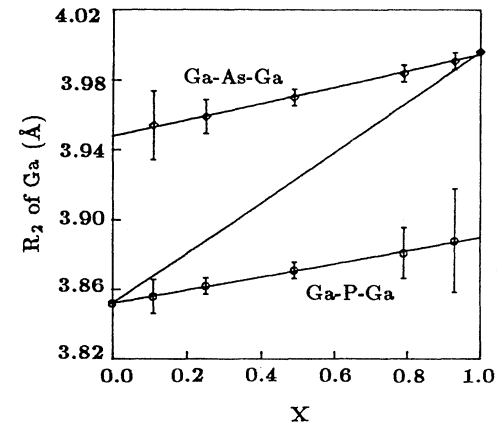

FIG. 5. Second-neighbor bond lengths of Ga in $GaAs_xP_{1-x}$ solid solution. Symbols denote the experimental results. The upper solid line is the fitting curve of $R_{Ga\text{-}As\text{-}Ga}$ and the lower solid line is the fitting curve of $R_{Ga\text{-}P\text{-}Ga}$. The middle line is the value indicated by VCA.

Our experimental results demonstrate that all the bond lengths increase with the content of As atoms and provide evidence of structural distortion in $GaAs_xP_{1-x}$ solid solutions. It is worthwhile to study how to accommodate these distortions and to understand the atomic-scale structure. The EXAFS results present an average effect of possible coordination structures. For zinc-blende-type AB_xC_{1-x} solid solutions, only five possible coordinations surround cation A with n ($n=0,1,2,3,4$) B-type anions and $4-n$ C-type anions. Assuming a random distribution of anions, the probability of finding a tetrahedron with n B-type anions for a composition X can be given by[9]

$$P(n,X)=\begin{bmatrix}4\\n\end{bmatrix}X^n(1-X)^{4-n}\ . \tag{5}$$

We assume that the near-neighbor atomic interaction is dominant and that we can neglect the effect of the complete disorder in further shells on the near-neighbor coordination structure. So for a certain coordination environment, the interatomic distances should be fixed. Therefore, there are five special tetrahedra in zinc-blende-type AB_xC_{1-x} solid solutions, which are packed following some rule to form the structure. For different compositions, the five tetrahedra are the same but their distribution is different and can be described by Eq. (5). In order to verify the above hypotheses, using the bond lengths obtained from EXAFS, a system of equations relating the special bond lengths $R^{(n)}$ of five such special tetrahedra to experimental values $R(X)$ can be set up:

$$R(X)=\frac{\sum_n W(n)P(n,X)R^{(n)}}{\sum_n W(n)P(n,X)}\ . \tag{6}$$

Here, n denotes n B-type and $4-n$ C-type anions at the vertices of the tetrahedron around cation A. $W(n)$ is the number of the corresponding bonds in such a tetrahedron. $R(X)$ is the bond length measured from EXAFS at composition X. The special bond lengths obtained from $GaAs_xP_{1-x}$ solid solutions as listed in Table V are obtained solving Eq. (6). They satisfy all the geometrical requirements of a tetrahedron.

It is obvious that the bond length $R_{\text{As-Ga}}$ around the As atom can also be described by using Eq. (6). This demonstrates that the tetrahedra with As and P anions at the centers and Ga cations at the vertices are also not regular ones in spite of the fact that the atoms at the vertices are the same. So the distances from the central As or P anions to the four Ga cations at the vertices are different. The same situation exists for the bond lengths $R_{\text{Ga-P-Ga}}$ and $R_{\text{Ga-As-Ga}}$. EXAFS results present the average effect of these distorted tetrahedra, and the respective occupancies of these tetrahedra are different and depend on the composition. This is why the bond lengths indicated by EXAFS vary with composition. From a geometrical point of view, all bond angles can be made to vary linearly with composition.

Although in $GaAs_xP_{1-x}$ solid-solution atoms deviate from the ideal lattice positions and construct five special tetrahedra, by averaging the five tetrahedra the regular one as implied by VCA can be obtained. Therefore, long-range order is still preserved as indicated by x-ray diffraction. It can be further concluded that EXAFS results are the average effect over the different coordination situations, and x-ray diffraction reflects the averaged EXAFS results.

In their structural model, Balzarotti *et al.*[9] assumed that the cation sublattice remains undistorted for $A_{1-x}B_xC$ alloy. This is obviously in conflict with the fact that the second-neighbor bond lengths $R_{A\text{-}C\text{-}A}$, $R_{A\text{-}C\text{-}B}$, and $R_{B\text{-}C\text{-}B}$ are different. We believe that the zinc-blende-type structure can be described by using the five special coordination tetrahedra for any composition, instead of five different tetrahedra for different compositions. This structural figure is succinct and the five special tetrahedra can be determined easily from the EXAFS results. Our model reflects a more reliable atomic-scale structure of zinc-blende-type solid solutions. To understand the stability of the structural model, theoretical considerations are necessary. The energetic calculation for this model will be presented in a future work.

The measurement of the elastic core effect is one of the direct verifications of the elastic theoretical model of solid solutions. The elastic core effect can be expressed with the following formula in the elastic continuous-medium theory (ECMT):[19]

$$\frac{da}{ac}=\frac{\nu db}{y}/b\left[1+\frac{(\nu-1)}{y}c\right]. \tag{7}$$

Here, $\nu=3(1-\sigma/1+\sigma)$, σ is a Poisson ratio, c is the atomic fraction of solute, b is the first-neighbor bond length of the solvent lattice, a is the lattice parameter, db and da are the variations of the first-neighbor bond length and lattice parameter, respectively, y is a parameter relative to the crystal structure, $y=3\Omega/(4\pi b^3)$, Ω is the mean volume of an atom in the solvent lattice.

Now we consider the cases of 7% and 1% GaP doping in GaAs. The lattice parameter of GaAs is 5.650 Å (80 K), the first-neighbor bond length b is 2.447 Å, and the Poisson ratio σ is 0.29.[20] For fcc $y=0.169$, for diamond, $y=0.368$, but for zinc-blende $GaAs_xP_{1-x}$ solid solutions, the GaAs molecule is displaced by the GaP molecule and y means the mean volume occupied by a molecule in a solvent lattice, so $y=0.735$. The lattice parameter of the solid solution with 7% GaP was measured to be 5.635 Å (80 K) and $da=-0.015$ Å. So $db^{\text{ECMT}}=-0.044$ Å, calculated using Eq. (7). But from the EXAFS measurement $db^{\text{EXAFS}}=-0.075$ Å, i.e., $db^{\text{EXAFS}}/db^{\text{ECMT}}\simeq 1.7$. For the solid solution with 1% GaP, the elastic core effect can also be evaluated from the fitting curve of the lattice parameter and $R_{\text{Ga-P}}$ obtained using the EXAFS technique, $db^{\text{EXAFS}}/db^{\text{ECMT}}\simeq 1.9$. Therefore, for the dilute solid solution of GaP in GaAs, the elastic core effect measured with EXAFS is almost twice as large as that calculated with ECMT. This is very similar to what is found in metal solid solutions.[19] It demonstrates that ECMT is inappropriate for describing the $GaAs_xP_{1-x}$ solid solutions. It seems that the ECMT also cannot correctly describe the local distortion of other zinc-blende solid solutions.

V. CONCLUSION

(1) In $GaAs_xP_{1-x}$ solid solutions, the near-neighbor bond lengths vary linearly with composition. The variation slope of the first-neighbor bond lengths with composition is about 18% of that calculated from Vegard's law. For the second neighbor, bond lengths of Ga ($R_{\text{Ga-As-Ga}}$ and $R_{\text{Ga-P-Ga}}$) are about 30%, and those of As ($R_{\text{As-Ga-As}}$

TABLE V. Bond lengths (in Å) of the five special tetrahedra of $GaAs_xP_{1-x}$ solid solutions (80 K).

n[a]	$R_{\text{Ga-As}}$	$R_{\text{Ga-P}}$	$R_{\text{As-Ga-As}}$	$R_{\text{As-Ga-P}}$	$R_{\text{P-Ga-P}}$
0		2.359			3.852
1	2.428	2.364		3.880	3.909
2	2.430	2.368	3.905	3.918	3.961
3	2.441	2.372	3.945	3.982	
4	2.446		3.996		
$W(n)$[b]	n	$4-n$	$0.5n^2-0.5n$	$-n^2+4n$	$0.5n^2-3.5n+6$

[a] n denotes n As and $4-n$ P anions at the vertices of a tetrahedron around a cation Ga.
[b] $W(n)$ is the number of the corresponding bond in such a tetrahedron.

and $R_{\text{As-Ga-P}}$) are greater than 65%, i.e., much closer to the VCA model.

(2) The lattice parameters of $GaAs_xP_{1-x}$ solid solutions vary linearly with composition and follow Vegard's law, as is also shown by the average value of all bond lengths. It can be concluded that the variation of the lattice parameters with composition comes from the contributions of all the different near-neighbor bond lengths.

(3) The zinc-blende-type structure can be described with five special coordination tetrahedra. EXAFS results reflect the average effect over those tetrahedra. In $GaAs_xP_{1-x}$ solid solutions, the Ga sublattice is relatively rigid and tends to remain equal to that in GaAs and GaP, while the mixed As, P sublattice is more flexible and approaches the VCA model. That implies a local structure distortion in the lattices of $GaAs_xP_{1-x}$ solid solutions.

(4) Describing the elastic core effect of $GaAs_xP_{1-x}$ solid solutions with elastic continuous medium theory is inappropriate.

ACKNOWLEDGMENTS

The authors wish to thank the Photon Factory in Japan for the use of the beamline and Dr. M. Nomura for assistance with the experiment. We also thank Xie Yaling, Hai Yong, Qiao Shan, and Hu Tiandao of the Institute of High Energy Physics, Chinese Academy of Sciences, for their assistance with the experiment and for the use of the beamline. This research was supported by the Chinese National Science Foundation and a grant from the State Science and Technology Commission of China (for key research project in Climbing Programme).

[1]M. B. Panish, J. Phys. Chem. Solids **30**, 1083 (1969).

[2]M. H. Pilkuhn and H. Rupprecht, Trans. Metall. Soc. AIME **230**, 282 (1964).

[3]J. A. Van Vechten and T. K. Bergstresser, Phys. Rev. B **1**, 3351 (1970).

[4]Y. Takeda, Sq. Fujita, and A. Sasaki, in *Growth and Properties of Constant Composition Bulk GaAsP Ternary Alloys,* Proceedings of the Eleventh International Symposium on Gallium Arsenide and Related Compounds, edited by B. de Cremoux, IOP Conf. Proc. No. 74 (Institute of Physics and Physical Society, London, 1984), Chap. 2 p. 23.

[5]A. Balzarotti, P. Letardi, and N. Motta, Solid State Commun. **56**, 471 (1985).

[6]A. E. Blakeslee, in *Perfection of Vapour Grown* $GaAs_{1-x}P_x$ *Superlattices,* Proceedings of the Third International Symposium on Gallium Arsenide and Related Compounds, edited by K. Paulus (assisted by F. E. Fawkes), IOP Conf. Proc. No. 9 (Institute of Physics and Physical Society, London, 1970), Chap. 5, p. 283.

[7]G. A. Antypas, R. L. Moon, L. W. James, J. Edgecumbe, and R. L. Bell, in *III-V Quaternary Alloys,* Proceedings of the Fourth International Symposium on Gallium Arsenide and Related Compounds, edited by C. Hilsum, IOP Conf. Proc. No. 17 (Institute of Physics and Physical Society, London, 1972), Chap. 1, p. 48.

[8]J. C. Mikkelsen, Jr. and J. B. Boyce, Phys. Rev. B **28**, 7130 (1983).

[9]A. Balzarotti, N. Motta, A. Kisiel, M. Zimnal-Starnawska, M. T. Czyzyk, and M. Podgorny, Phys. Rev. B **31**, 7526 (1985).

[10]P. Letardi, N. Motta, and A. Balzarotti, J. Phys. C **20**, 2853 (1987).

[11]W. F. Pong, R. A. Mayanovic, B. A. Bunker, J. K. Furdyna, and U. Debska, Phys. Rev. B **41**, 8440 (1990).

[12]Toru Sasaki, Tomohiro Onda, Ryoichi Ito, and Nagaatsu Ogasawara, Jpn. J. Appl. Phys. **25**, 231 (1986).

[13]James J. Tietjen and Jannes A. Amick, J. Electrochem. Soc. **113**, 724 (1966).

[14]D. E. Sayers and B. A. Bunker, in *X-ray Absorption: Principles, Applications and Techniques of EXAFS, SEXAFS and XANES,* edited by D. C. Koningsberger and R. Prins (Wiley, New York, 1988), Chap. 6.

[15]F. W. Lytle, D. E. Sayers, and E. A. Stern, Physica B **158**, 701 (1989).

[16](a) J. J. Rehr, J. Mustre de Leon, S. I. Zabinsky, and R. C. Albers, J. Am. Chem. Soc. **113**, 5135 (1991); (b) J. Mustre de Leon, J. J. Rehr, S. I. Zabinsky, and R. C. Albers, Phys. Rev. B **44**, 4146 (1991).

[17]J. B. Boyce and J. C. Mikkelsen, Jr., Phys. Rev. B **31**, 6903 (1985).

[18]Lu Kunquan, Wu Zhonghua, Dong Jun, Chen Xinping, and Fang Zhengzhi, Sci. China A **4**, 390 (1992).

[19]D. Raoux, A. Fontaine, P. Lagarde, and A. Sadoc, Phys. Rev. B **24**, 5547 (1981).

[20]N. A. Goryunova, *The Chemistry of Diamond-Like Semiconductors,* edited by J. C. Anderson (MIT, Cambridge, MA, 1965), p. 236.